

# Analysis of transients in the medium voltage supply circuit of a high-current laboratory

JOLANTA SADURA <sup>1</sup>✉, JAN SROKA <sup>1</sup>, JACEK STARZYŃSKI <sup>2</sup>

<sup>1</sup>*Institute of Theory of Electrical Engineering, Measurement and Information Systems  
Warsaw University of Technology  
Pl. Politechniki 1, 00-661 Warsaw, Poland*

<sup>2</sup>*Faculty of Electronic  
Military University of Technology  
ul. gen. Sylwestra Kaliskiego 2, 00 – 908 Warsaw 46, Poland  
e-mail: [[✉ jolanta.sadura@jan.sroka](mailto:jolanta.sadura@jan.sroka@pw.edu.pl)]@pw.edu.pl, [jacek.starzynski@wat.edu.pl](mailto:jacek.starzynski@wat.edu.pl)*

(Received: 13.08.2025, revised: 29.01.2026)

**Abstract:** Electric and magnetic field measurements performed in the high-current laboratory (HCL) revealed recurring disturbances in the form of damped oscillations. An analysis of the test procedures and a detailed investigation of the system configuration indicated that the likely cause of these disturbances was the asynchronous operation of contacts in a medium-voltage (MV) vacuum circuit breaker. This hypothesis was verified using both field and circuit simulations. The non-uniform test circuit of the HCL was represented as a cascaded equivalent model based on segmentation and distributed electrical parameters. The obtained simulation results confirmed the proposed hypothesis and highlighted the significant impact of the switching process on the generation of electromagnetic disturbances in the MV supply path.

**Key words:** circuit segmentation, damped oscillations, electromagnetic disturbances, high-current laboratory, MV vacuum circuit breaker, partial parameters of the supply circuit

## 1. Introduction

In modern high-current laboratories (HCLs), where short-circuit tests and dielectric strength assessments of power system equipment are performed, the control and interpretation of transient phenomena occurring in power supply circuits represent a critical aspect of system operation.



© 2026. The Author(s). This is an open-access article distributed under the terms of the Creative Commons Attribution-NonCommercial-NoDerivatives License (CC BY-NC-ND 4.0, <https://creativecommons.org/licenses/by-nc-nd/4.0/>), which permits use, distribution, and reproduction in any medium, provided that the Article is properly cited, the use is non-commercial, and no modifications or adaptations are made.

A significant challenge arises from the non-uniformity of current paths and the switching devices integrated into them, such as vacuum circuit breakers (CBs). This structural and functional complexity makes it difficult to accurately identify and analyse the sources of repetitive electromagnetic disturbances, particularly those in the form of damped oscillatory waves (DOWs).

The electromagnetic environment of the short-circuit testing laboratory differs significantly from those defined in standardised environments. In [8] three different EMC environments are defined, for: power stations, air insulated substations and gas insulated substations. Each environment is subdivided into areas. For this paper, the control area is of prime importance. Only for equipment intended for control the area in substations, an immunity test against DOWs is required.

The electromagnetic compatibility (EMC) environment of the HCL varies from those defined in [8] due to the lack of a high-voltage (HV) area. Instead, it possesses a high-current area. Moreover, control areas in power stations and in substations are separate buildings, unlike in the HCLs where all areas i.e.: MV, control and high current areas are situated in the same building, without any electromagnetic barriers between them. These increases the risk of more severe DOWs in the HCL.

There are no technical and scientific publications explaining origin of DOWs and what is more important their repetitive character. [9] is devoted to EMC in power plants and substations. In chapter 6.1.1.4, it is merely mentioned that oscillatory transients emulate disturbances accompanying HV isolator switching, circuit breaker switching and faults. The aim of this paper is to find the answer on both questions concerning DOWs in the HCL, i.e. their origin and repetitive character.

The presence of such oscillations, especially when triggered by unintended pulses during the switching process, can lead to unexpected current surges and pose a threat to both equipment and personnel. Sudden, uncontrolled initiation of short-circuit test procedures introduces real hazards to human life and the integrity of high-value test objects.

To address the analytical difficulties posed by non-uniform supply paths, the approach proposed in this work involves segmentation of the power circuit into discrete blocks with approximately homogeneous current paths. This allows the assignment of local electrical parameters, such as inductance and capacitance to each segment. The segmented model is then used in circuit simulations to assess how individual elements, especially switching devices, influence overall transient response of the system, especially voltage transients.

The paper presents the analysis of repetitive damped oscillations observed during the operation of a medium-voltage vacuum CB in the HCL. The closing process is presumed to be the origin of it. This hypothesis is validated by means of numerical simulation.

## 2. Description of the analysed system: power supply circuit of the high-current laboratory

The electric scheme of the laboratory setup is shown in Fig. 1. In the MV supply line a vacuum circuit breaker (MV CB) accompanied by current limiting inductors (CLIs) is mounted. Three single-phase test transformers (TTs) load the line, and can be connected as required. In the high current area, there are short circuit switches (SCSs) responsible for starting and finishing tests. CBs and SCSs are controlled with the switches' controller.

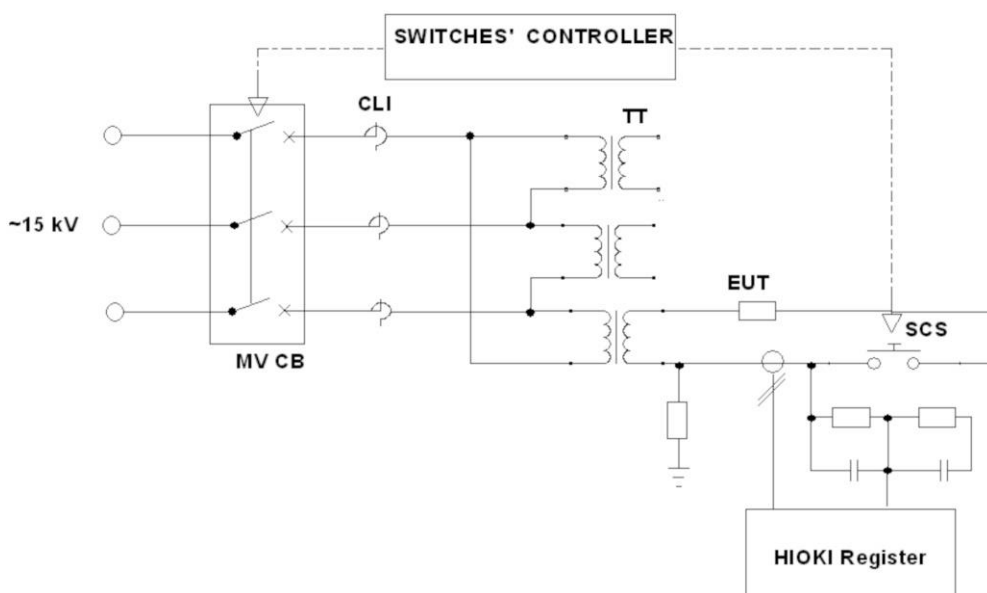


Fig. 1. Electrical circuit of the test system for short-circuit strength tests

Numerical simulations are performed for transients generated by closing the MB CB while SCSs are opened.

Initial measurements of the electromagnetic environment using directional electric and magnetic field probes (B-dot and D-dot) as well as  $E$ ,  $H$  probe allowed for a clear identification of disturbances as repetitive, damped oscillations occurring during energizing the primary side of the test transformer (TT). The probes were situated next to the switches' controller. B-dot and D-dot probes are products of MONTENA Technology SA. They are free space directional probes with the frequency bandwidth 1 GHz and 2.5 GHz, respectively.  $E$ ,  $H$  probe is the product of MASCHEK Elektronik. It is isotropic with a frequency bandwidth from 5 Hz to 400 kHz.

During measurements of electric and magnetic fields, voltages were also monitored. Namely, directly across the unloaded (no-load) secondary side of the TT and at the terminals of the switches' controller. The results, including an electric field strength of approximately 530 V/m and a magnetic field strength of 0.4 A/m, indicate that the source of the interference is of electric origin. Based on the recorded signals, it was hypothesised that the source of disturbance lies in the vacuum circuit breaker installed in the power supply paths.

Therefore, the scope of further analysis was narrowed to the selected part of the test system, the segment located on the primary side of the test transformer, which plays a critical role in initiating the disturbances. Furthermore, independent laboratory testing of the vacuum circuit breaker (dismounted from the system) confirmed a lack of synchronism in contact closure across its individual poles.

In Fig. 2 as well in Fig. 3 double damped oscillatory waves are recorded.

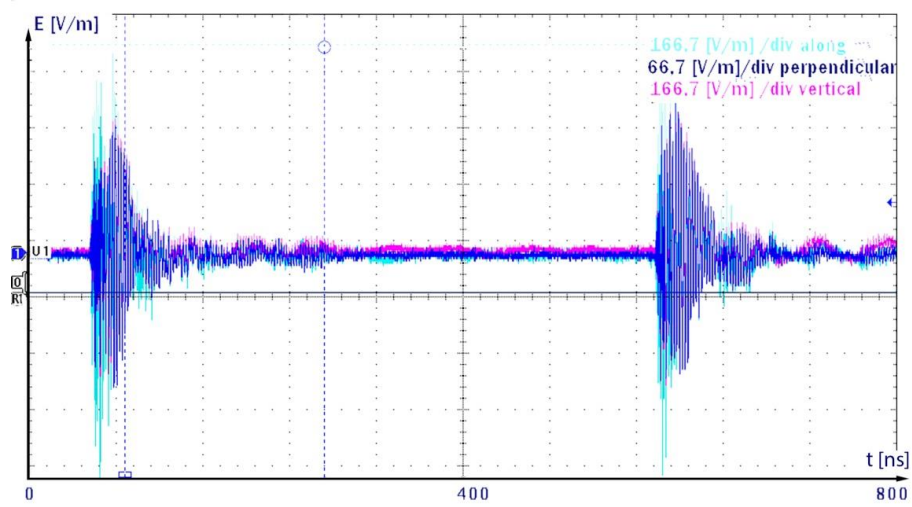


Fig. 2. Electric field measured with the Maschek isotropic probe

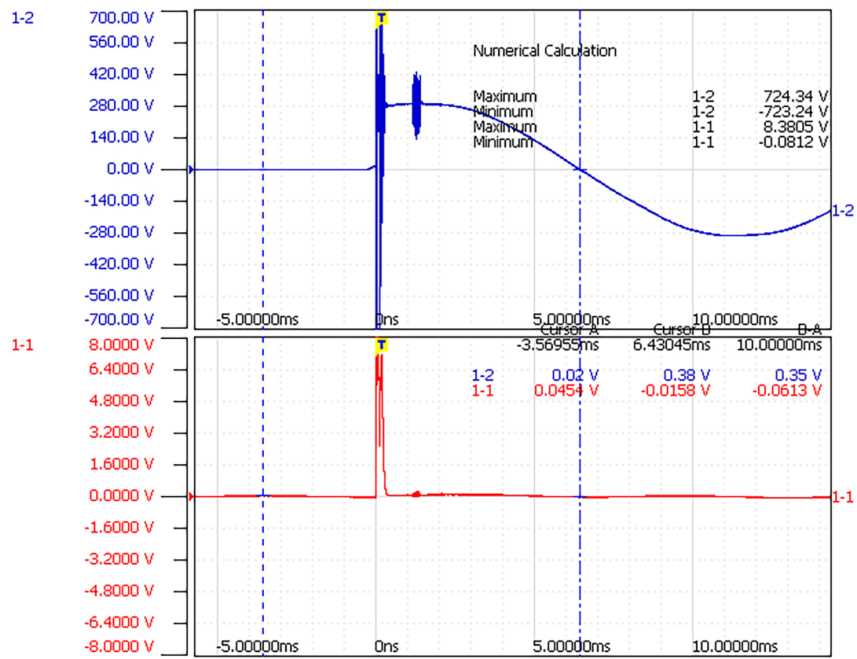


Fig. 3. Voltage transients on the LV side of the unloaded TT (blue) and on the contacts of the relay of the switches' controller (red)

### 3. Current paths configuration and calculation of partial parameters

The presented layout of current paths is very complex as shown in Fig. 4, and his general character is modeled as shown in Fig. 5. It possesses partial capacitance and inductances matrices, which include both self and mutual capacitances and inductions. The results of the performed simulations, both field-based and circuit-level, refer to the actual, non-uniform distribution of current paths occurring in the HCL.

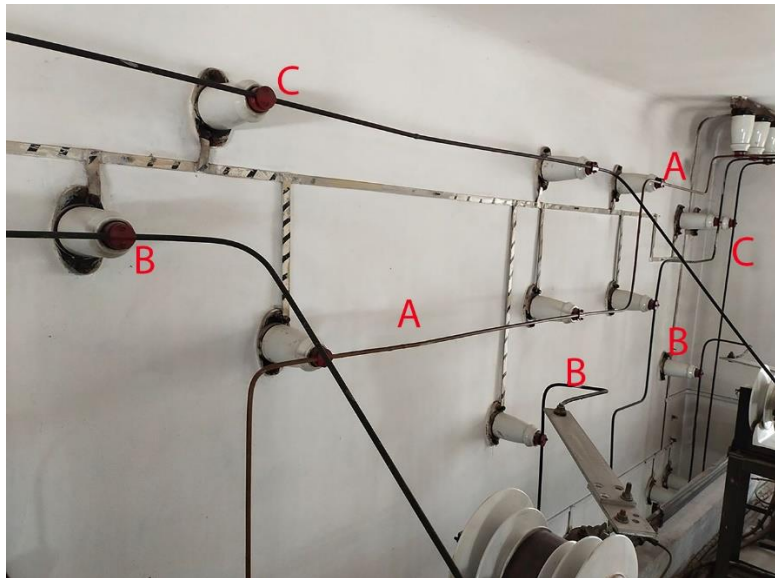


Fig. 4. The non-uniformity current tracks close to the CB switch

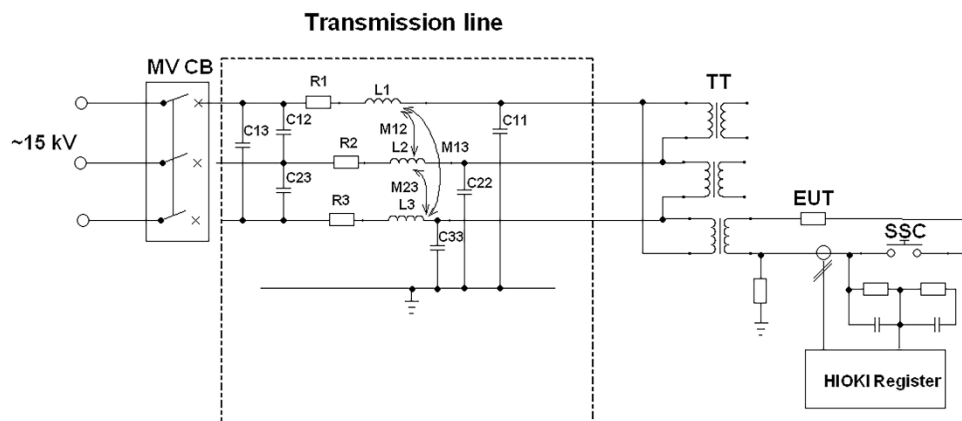


Fig. 5. Simplified schematic of the simulation model of the test circuit

Due to the varying geometry of the analysed system, a series of field simulations were carried out to determine the circuit parameters, namely inductance ( $L$ ), capacitance ( $C$ ), and resistance, for individual sections of the system (in this case, three sections). These current path segments can be considered as portions with approximately constant parameters, which enabled their segmentation for use in the circuit model.

The power current path for each phase exhibits geometric non-uniformity, including different orientations related to other paths, to the reference planes (e.g. wall and ceiling as presented in Fig. 6), and to nearby conductive elements. Based on comprehensive geometric data, including cross sections and distances between conductors, a series of field simulations were performed to determine the self- and mutual capacitances of the system.

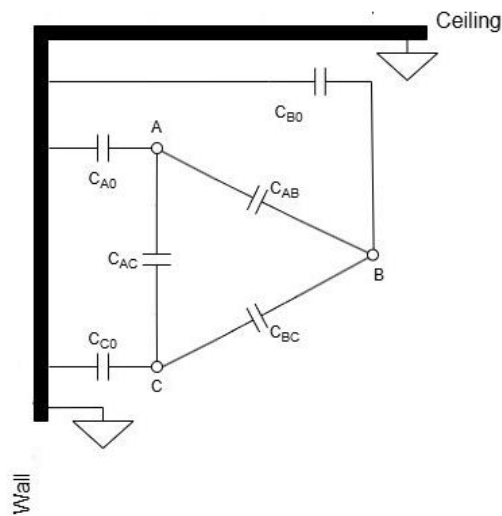


Fig. 6. Cross-sectional layout of the segment of the MV supply current paths with corresponding set of capacitances

The simulations used energy distribution methods and the relation to calculate the partial capacitance matrix, which was then used to obtain the global capacitance matrix [3]. In the same manner, the inductance matrix can be calculated.

However, it should be noted that extracting inductance values directly from field simulations is not feasible for highly complex test circuits, because of the undefined nature of the return current paths and the inability to model current density distributions within the reference ground mass.

Using the calculated parameters for the most homogeneous segments of the current paths, a simplified equivalent circuit was constructed. This model divides the power circuit into three sections that can be treated as electrically uniform for the purposes of transient simulations. In the first and the second ones, conductors are laid out parallel to the wall. In the third one, parallel to the ceiling.

To determine three self and three mutual partial capacitances, it is necessary to perform six numerical simulations for each section.

An exemplary simulation of potential distributions for the segment where all paths are in the plane parallel to the wall is presented in Figs. 7(a), 7(b), and 7(c).

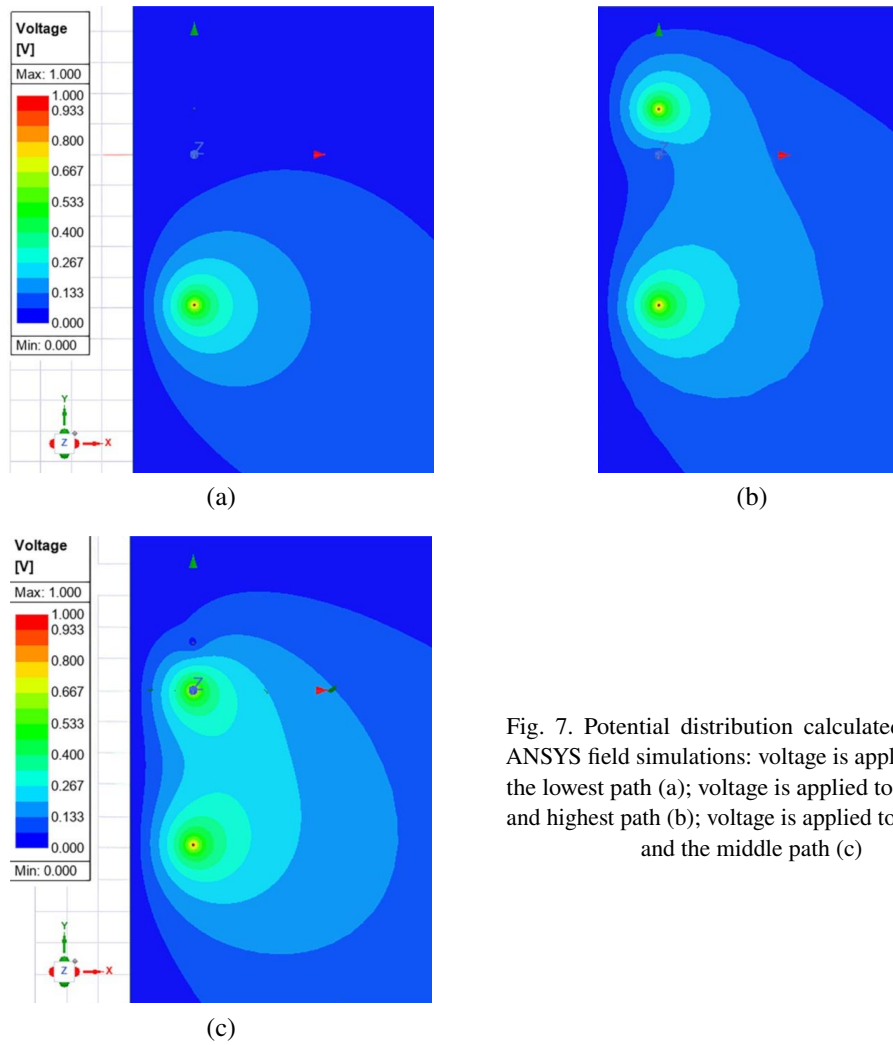


Fig. 7. Potential distribution calculated with the ANSYS field simulations: voltage is applied only to the lowest path (a); voltage is applied to the lowest and highest path (b); voltage is applied to the lowest and the middle path (c)

$$\begin{bmatrix} 1 & 1 & 1 & 0 & 0 & 0 \\ 0 & 0 & 1 & 0 & 1 & 1 \\ 0 & 1 & 0 & 1 & 0 & 1 \\ 1 & 0 & 0 & 1 & 1 & 0 \\ 1 & 0 & 1 & 1 & 0 & 1 \\ 1 & 1 & 0 & 0 & 1 & 1 \end{bmatrix} \begin{bmatrix} c_{A0} \\ c_{B0} \\ c_{C0} \\ c_{AB} \\ c_{CA} \\ c_{BC} \end{bmatrix} = \frac{2}{U^2} \begin{bmatrix} W_{ABC} \\ W_C \\ W_B \\ W_A \\ W_{CA} \\ W_{BC} \end{bmatrix}. \tag{1}$$

Indexes by energy denote the paths to which voltage is applied.

From the partial capacitance present in Eq. (1) a square matrix of global capacitances can be built.

$$C = \begin{bmatrix} c_{A0} + c_{AB} + c_{AC} & -c_{AB} & -c_{AC} \\ -c_{BA} & c_{B0} + c_{BA} + c_{BC} & -c_{BC} \\ -c_{CA} & -c_{CB} & c_{C0} + c_{CA} + c_{CB} \end{bmatrix}. \quad (2)$$

According to [3] and [12], the product of global inductance and capacitance matrixes  $L$  and  $C$  is equal to the product of magnetic permeability  $\mu$  and dielectric permittivity  $\varepsilon$ .

$$LC = \mu\varepsilon\mathbf{1}_3, \quad (3)$$

where  $\mathbf{1}_3$  is a  $3 \times 3$  identity matrix defined as having unity entries on the main diagonal and zeroes elsewhere.

$$\mathbf{1}_3 = \begin{bmatrix} 1 & 0 & 0 \\ 0 & 1 & 0 \\ 0 & 0 & 1 \end{bmatrix}. \quad (4)$$

Equation (3) enables to calculate inductance matrix  $L$  from capacitance matrix  $C$  determined in numerical simulations.

$$L = \mu\varepsilon C^{-1}. \quad (5)$$

In the equivalent circuit of the test transformer TT magnetisation losses and magnetisation inductance are taken into account, as it is usual for an unloaded transformer.

#### 4. Transient simulations

The electrical scheme of the circuit simulated numerically is shown in Fig. 8. Three segments of the current paths are shown there. Two of them W1 and W2 are situated in the plane parallel to the wall. The third one C, is parallel to the ceiling. The third segment is terminated with the test transformer whose phases are connected in delta. Each transformer phase is modeled with parallel branches of magnetisation inductance and losses. Both of them are assumed to be linear.

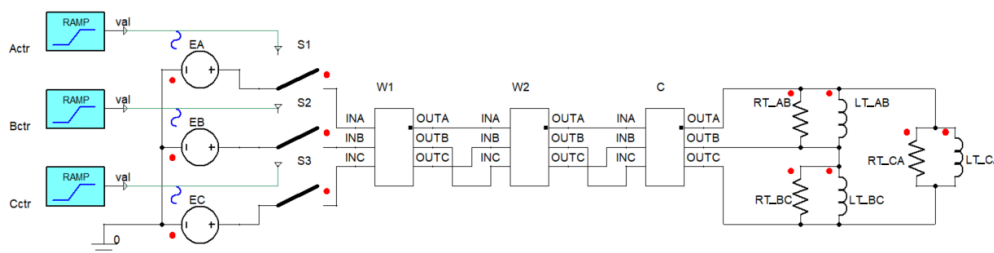


Fig. 8. Electrical circuit model for transient simulations with ANSYS. All segments are modelled with lumped circuits

A series of simulations were carried out to study the transient behavior of the segmented circuit under varying assumptions for the closing time delays of the vacuum circuit breaker contacts, ranging from nanoseconds to several milliseconds.

The phenomenon of asynchronous contact closing exhibits repetitive damped oscillations reaching frequencies up to 5 MHz, which corresponds to a wavelength of approximately 60 m. The first two segments of the power paths are shorter than 3 m. The third segment is longer than 8 m. It is uncontroversial to model the first two segments as lumped circuits. In the first approach, the third segment was modeled as a lumped circuit as well. The results of such simulations are presented in Fig. 9, Fig. 10 and Fig. 11. In Fig. 9, two contacts are closed in the same instant 0 ms and the third with 80  $\mu$ s delay.

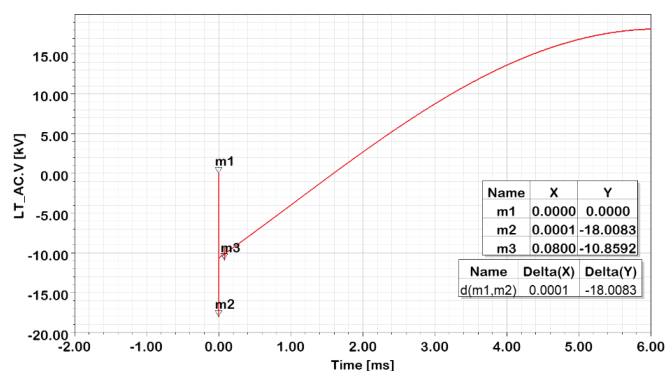
In Fig. 10, again, two contacts are closed in the same instant, 0 ms, and the third with a delay of 800 ns delay. In the waveform in Fig. 10(a), the low frequency transient is visible. Such transients are reported in [4]. The envelope of the second oscillation in Fig. 10(b) has a complex character differing from the envelope with one attenuation coefficient. It is due to overlapping of two transients.

In Fig. 11, all contacts are closed in different instants 0 ms, 80  $\mu$ s and 5 ms.

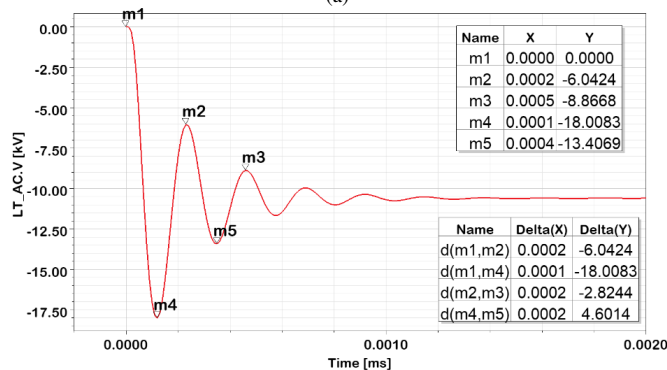
In all simulations, the number and instant of DOWs' initiations correspond with a sequence of contact closing in the MW CB, while the first transient is most severe.

Because the length of the third segment is comparable to the wavelength, it was also modeled as a distribution line discretized with four rungs of the ladder network, as shown in Fig. 12.

The results of these simulations, in which two contacts were closed in the same instant, 0 ms, and the third with an 80  $\mu$ s delay, are presented in Fig. 13.



(a)



(b)

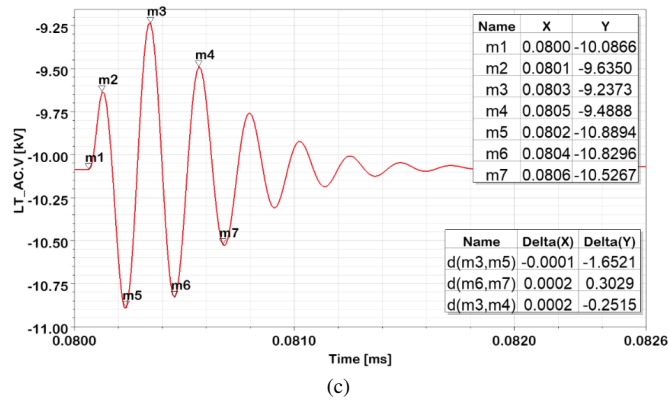


Fig. 9. Simulation results for the case of a contact closing delay in phase B of 80  $\mu$ s relative to the other phases

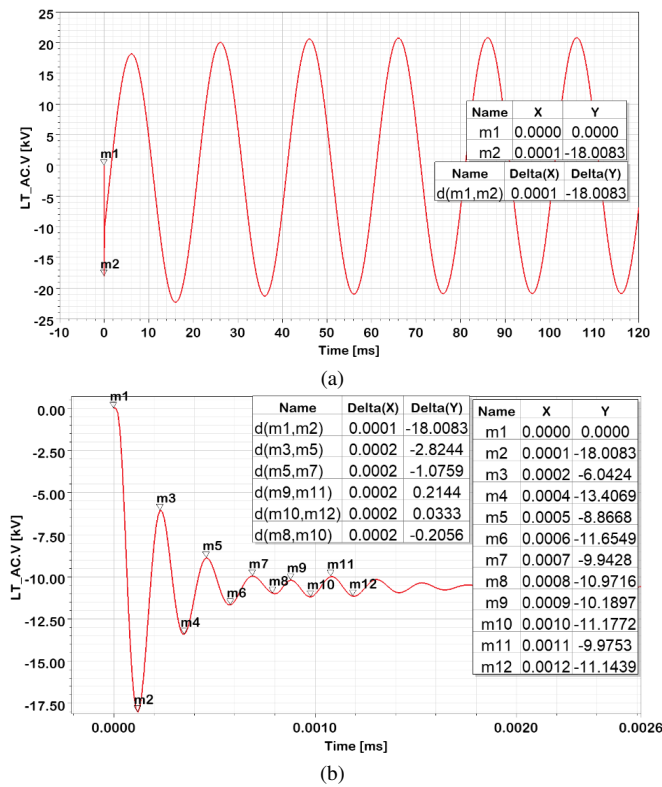


Fig. 10. Simulation results for the case of a contact closing delay in phase B of 800 ns relative to the other phases. Superimposed oscillations caused by the asynchronous closing of contacts are visible in (b)

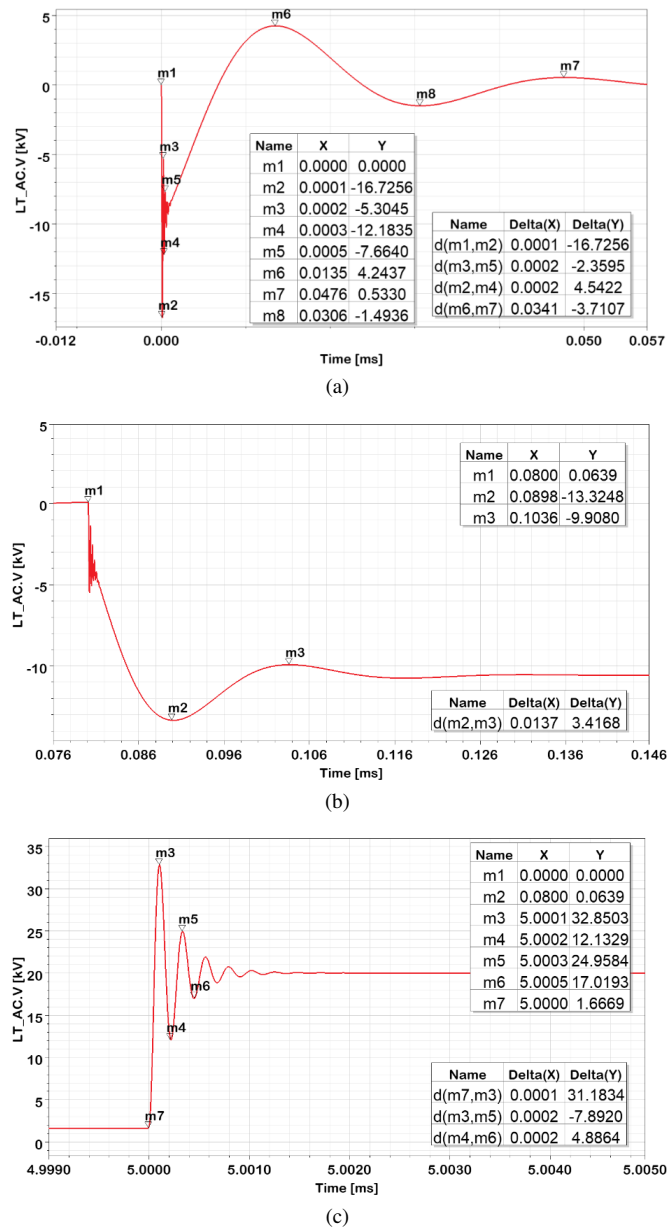


Fig. 11. Simulation results for the case with different closing instants in all phases: 0 ms, 80  $\mu$ s and 5 ms

In all simulations, Fig. 9(b), Fig. 10(b), Fig. 11(b) and Fig. 13(c), the first amplitudes of oscillations have values between 16 kV and 20 kV. This corresponds to a very big electric field, which exists in the HCL electromagnetic environment (Fig. 2).

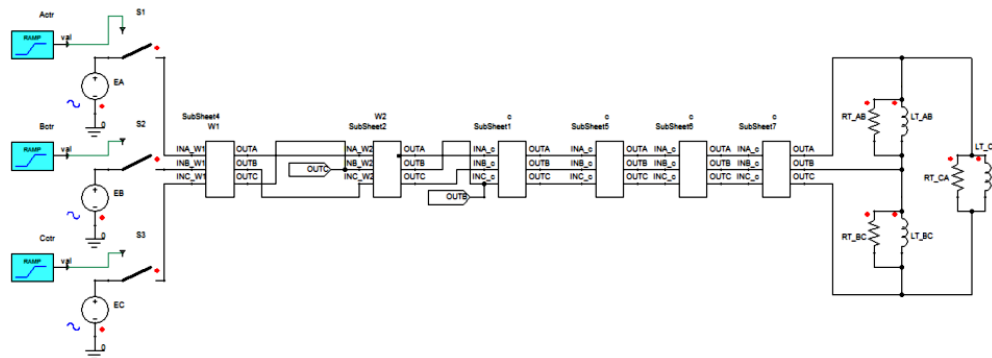
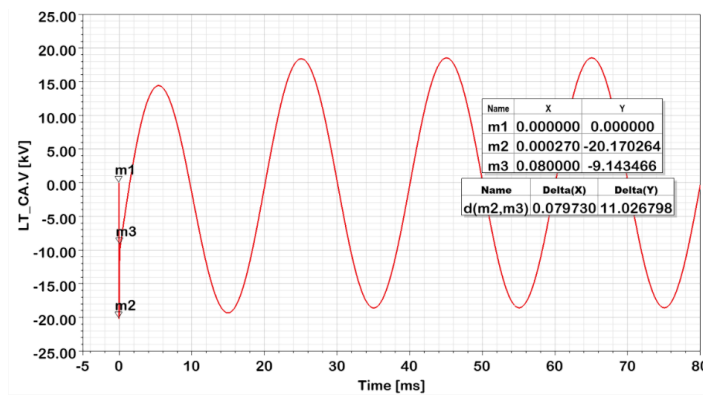
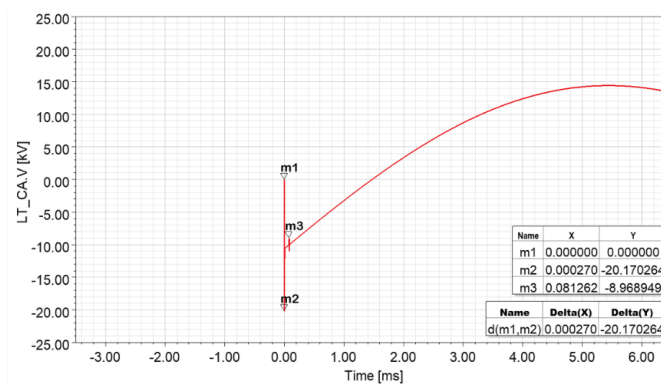


Fig. 12. Electrical circuit model for transient simulations with ANSYS. The third segment is modelled with four rungs of the ladder network

The comparison of the plots in Fig. 9 and Fig. 13 leads to the conclusion that replacing the lumped circuit of the third segment of the current paths with a distributed line, modeled with the ladder circuit decreases attenuation of oscillations.



(a)



(b)

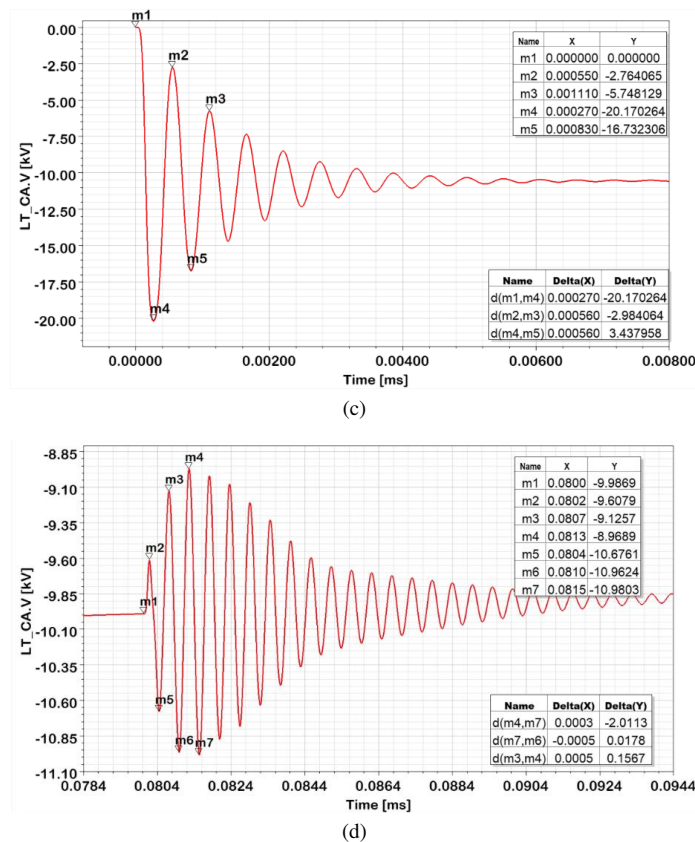


Fig. 13. Simulation results for the case of a contact closing delay in phase B of 80  $\mu$ s relative to the other phases: view of the first four periods (a); zoom on both transients (b) and zoomed the first (c) and the second (d) damped oscillations

The envelope of the second oscillations visible in Fig. 13(d), similarly to that in Fig. 9(c), has a complex character.

## 5. Conclusions

Asynchronous closing of contacts in the medium-voltage vacuum circuit breaker mounted in the supply circuit of the high-current laboratory is a significant source of repetitive damped oscillatory waves. Such oscillations are observable in voltages as well as in electric and magnetic fields in the electromagnetic environment of the laboratory.

The level (amplitude) of these disturbances is strongly dependent on the phase angle at which the circuit is energized.

Repetitive damped oscillations constitute a dominant feature of the electromagnetic environment within the high-current laboratory.

The electromagnetic environment of the short-circuit testing laboratory differs significantly from those defined in standardised environments such as [8] for power station and substation environments.

As it was stated in the Introduction, the EMC environment of the HCL varies from those defined in [8] and there exists a risk of more severe DOWs in the HCLs than in power stations or substations.

In the Introduction, the lack of technical and scientific publications explaining the origin of DOWs and, what is more important, their repetitive character, is reported. The novelty of this paper lies in answering the question about the origin of repetitive damped oscillations in the HCL. The finite closing time of circuit breaker contacts and a delay of the switching process in each path of the circuit breaker cause repetitive DOWs. It is proved with a numerical simulation of transients in the MV supply path by switching the circuit breaker.

Per length capacitances of the current paths are derived in this paper from the distribution of a static electric field calculated with ANSYS.

The simulations used energy distribution methods and the relation to calculate the partial capacitance matrix, which was then used to obtain the global capacitance matrix [3].

However, extracting inductance values directly from field simulations is not feasible in the presented case, because of the undefined nature of the return current paths and the inability to model current density distributions within the reference ground mass. Therefore, identity between the product of inductance and capacitance matrixes  $L$  and  $C$ , and the product of magnetic permeability  $\mu$  and dielectric permittivity  $\varepsilon$  was applied for the calculation of the per length inductance matrix  $L$  [3].

The model for numerical simulations of the current supply paths must be carefully treated due to its character: a lumped circuit or circuit with distributed parameters. Simulations with exclusively lumped circuits as well as distributed parameters contain low-frequency transients, which are reported in the literature [4].

In all simulations, the number and instant of DOWs' initiations correspond with the sequence of contact closing in the MW CB, while the first transient is most severe.

Replacing the lumped circuit of the third segment of the current paths with a distributed line modeled with the ladder circuit decreases the attenuation of oscillations.

## References

- [1] Sadura J., Sroka J., Owsiniński M., Jósko A., *Identification of EM disturbances interfering the time-phase controller by short circuit tests*, Proceedings of the 2020 International Symposium on Electromagnetic Compatibility – EMC EUROPE, EMC EUROPE 2020, Rome (2020).
- [2] Sadura J., Sroka J., Sul P., Jósko A., Owsiniński M., *Susceptibility Issues of Control Instrumentation in Electromagnetic Environment of High Current Laboratory*, Energies, vol. 15, no. 13, pp. 1–13, 4682 (2022), DOI: [10.3390/en15134682](https://doi.org/10.3390/en15134682).
- [3] Paul C.R., *Analysis of Multiconductor Transmission Lines*, 2nd ed. John Wiley & Sons, ISBN 978-0-470-13154-1 (2007).
- [4] Nowicki J., Maksymiuk J., *Electrical apparatus and switchgears high and medium voltages*, Oficyna Wydawnicza PW (in Polish), ISBN 9788378141754, Warszawa (2014).
- [5] Sroka J., *Compendium on ElectroMagnetic Compatibility*, WUT Publishing House, ISBN 978-83-8156-276-8 (print), ISBN 978-83-8156-277-5 (online), Warsaw (2021).

- [6] Kiszło S., *Medium voltage switches, construction, research, operation*, Instytut Energetyki, Warszawa (in Polish), ISBN 978-83-63226-22-0, Warsaw (2020).
- [7] IEC 61000-4-18, *Electromagnetic compatibility (EMC) – Part 4–18: Generic standards – Testing and measurement techniques – Damped oscillatory wave immunity test* (2019).
- [8] IEC 61000-6-5, *Electromagnetic compatibility (EMC) – Part 6–5: Generic standards – Immunity for equipment used in power station and substation environment* (2015).
- [9] CIGRE 535, *EMC within Power Plants and Substations*, Working Group C4.208, ISBN: 978-2-85873-229-6 (2013).
- [10] KATKT10008, *MV vacuum circuit breaker Evolis*, <http://www.schneider-electric.pl> (2004).
- [11] Young M., *The Technical Writer's Handbook*, Mill Valley, CA: University Science (1989).
- [12] Sadura J., *Electromagnetic compatibility of the test control apparatus in environment of high-current laboratories*, WUT Publishing House (2024).